Physicochem. Probl. Miner. Process., 58(6), 2022, 155277

http://www.journalssystem.com/ppmp

Physicochemical Problems of Mineral Processing

ISSN 1643-1049

Characterization of perlite powders from Izmir, Türkiye region

Özay Aksoy [1], Elif Alyamaç [2,3], Merve Mocan [4], Mücahit Sütçü [5], Nihan Özveren-Uçar [6], M. Özgür Seydibeyoğlu [3,5]

[1] Biocomposites Engineering Graduate Program, Graduate School of Natural and Applied Sciences, Izmir Katip Çelebi University, 35620, Çiğli, Izmir, Türkiye

[2] Department of Petroleum and Natural Gas Engineering, Izmir Katip Çelebi University, 35620 Çiğli, Izmir, Türkiye

[3] Advanced Structures and Composites Center, University of Maine, 04469 Orono, ME, USA

[4] Department of Materials Science and Engineering, Gebze Technical University, 41400 Gebze, Kocaeli, Türkiye

[5] Department of Materials Science and Engineering, Izmir Katip Çelebi University, 35620 Çiğli, Izmir, Türkiye

[6] Materials Science and Engineering Graduate Program, Graduate School of Natural and Applied Sciences, Izmir Katip Çelebi University, 35620 Çiğli, Izmir, Türkiye

Corresponding author: elif.alyamac.seydibeyoglu@ikcu.edu.tr (Elif Alyamaç-Seydibeyoğlu)

Abstract: Perlite is an amorphous volcanic glass-type rock which is collected in open mines in various parts of the world. In this study, eight different perlite samples, supplied from the mines located in the Bergama, Izmir region, were used. The perlite samples were structurally, morphologically, and mineralogically characterized via a wide range of analytical techniques such as Thermogravimetric Analysis (TGA), Fourier Transform Infrared Spectroscopy (FTIR), Brunauer-Emmett-Teller (BET) Surface Area Analysis, Optical Microscopy, Scanning Electron Microscopy (SEM), X-ray Diffraction (XRD), X-ray Fluorescence (XRF), and a liquid pycnometer. Platelet shaped-like structures were observed in the SEM analysis of the expanded perlites in contrast to the images of spongy or cracked expanded perlites reported in literature. The O-H bending and Si-O-Si vibrations (both asymmetric and symmetric stretching) of perlite structures were confirmed by FTIR. Highly amorphous phases with a rather low percentage of crystalline phases were observed by XRD. In the BET surface area analysis, expanded perlite materials exhibited higher surface area compared to unexpanded ones. A detailed characterization of perlite structures is essential as there is a significant potential to use these minerals in various biocomposite applications and it is useful to explain structure-property relationships in this class of materials.

Keywords: perlite, characterization, expanded perlite, particulate morphology, mineralogy

1. Introduction

Perlite is a type of volcanic rock, that generally contains more than 60% alumina and silica contents (Barker et al., 2006; Gül, 2016; Haery, 2017). The name is derived from the word "perle", meaning pearl, due to the observed pearl brightness when broken into small spheres. Perlite differs from other volcanic glasses in that its volume expands 4-20 times of its original volume when heated quickly to 760–980 °C (Torab-Mostaedi et al., 2010; Maxim et al., 2014; Gül, 2016), transforming crushed perlite into a highly porous, low density, white form, named expanded perlite. Commonly, the term perlite is used for both the raw and expanded form. Perlite has many industrial applications due to its low thermal conductivity (Chen et al., 2020), high sound absorption and high thermal stability (Yilmazer and Ozdeniz, 2005), chemical inertness (Papadopoulos et al., 2008), and stiffness (Haery, 2017). It is also used in soilless agriculture because of its water retention property (Jamei et al., 2011). Small differences were observed between perlites from the east and west regions of the Türkiye (Erdem et al., 2007). Although these perlites look similar, mines could have differences in some aspects, as analysed with X-ray Fluorescence (XRF). Despite its industrial importance worldwide (www.perlite.org, 2022), only a few studies (Kabra et al., 2013; Celik et al., 2013) focused on the characterization of perlites.

DOI: 10.37190/ppmp/155277

In this study, perlites, obtained from the mines operated in the Izmir Bergama region of Türkiye, were selected and analyzed with many characterization techniques that had existed in literature (Kabra et al., 2013; Celik et al., 2013).

In the present study, a methodologically comprehensive approach to describe eight different perlite samples from the Bergama Izmir region, was used. In contrast to previously published studies, the samples were analyzed using a wide range of analytical techniques to provide the most extensive characterizations of perlite. Here we present data for numerous critical material-defining parameters, including Liquid Pycnometry, Analysis (TGA), Fourier Transform Infrared (FTIR) Spectroscopy, Brunauer-Emmett-Teller (BET) Surface Area Analysis, Optical Microscopy, Scanning Electron Microscopy (SEM), X-ray Diffraction (XRD), and X-ray Fluorescence (XRF), enabling a direct comparison between different samples as well as those reported in the literature.

The industrial importance of perlite is increasing. It is primarily used as a novel reinforcement and filler material in polymer composites which acts as a sound absorption material in the automotive industry (Dellock et al., 2020). In future research, the herein described perlite samples are planned to be used to manufacture perlite reinforced polymeric biocomposites. As a basis for such developments, a detailed and comprehensive material characterization is useful to explain the final material properties.

2. Materials and methods

2.1. Materials

Agricultural-expanded "a", coarse-expanded "b", fine-expanded "c", M1-expanded "d", M3-expanded "e" trade named perlites were in expanded forms. Coarse-unexpanded "f", fine-unexpanded "g", and micronized-unexpanded "h" are trade names for "pre-processed" perlites. Pre-processing, which is crushing of perlites into smaller particles, occurs in a second factory after mine. Then, "f,g,h" pre-processed perlites are manufactured in third perlite expansion and processing factory. The grain sizes of coarse, fine, and micronized unexpanded perlites range between 40 and 500 μm, 150 and 600 μm, up to 150 μm (this sample was pulverized), respectively. In this research, expanded perlites were pulverized in the laboratory. As a result, this would help expanded perlites to be shaped to platelet/flake form. The physical, chemical, morphological, and thermal analyses of eight perlite samples were done after receiving from the manufacturer 'Kale Perlit' (www.kaleperlit.com.tr, 2022). Details for the characterization of perlite materials were provided in the Methods section.

2.2. Methods

Whole-rock geochemical composition was obtained using a Spectro IQ II X-ray fluorescence (XRF) spectrometer in Iztech, Center for Materials Research,Urla, Izmir, Türkiye.

A Bruker D-8 Advance X-ray diffractometer was used to determine crystalline phase structure with Cu Kα radiation (40 kV, 40 mA) with a 0.01973° step over the range $5° < 2\theta < 65°$. The acquired diffractograms were interpreted with the aid of "X'Pert HighScore Plus" software.

Microscopic observations of the perlite samples were performed using a Nikon Eclipse LV150 polarising microscope with bright field mode. It's metallography microscope that images with reflection method were taken. Secondary electron images of gold coated samples were acquired using a PHILIPS XL 30S FEG with an accelerating voltage of 10 kV.

XRD, Optical Microscopy, SEM tests were conducted in laboratories in the Department of Materials Science and Engineering, Gebze Technical University, Gebze, Kocaeli, Türkiye.

The true density of powdered samples was measured with a 50 mL liquid pycnometer in Filinia R&D Company Laboratory, Bornova, Izmir, Türkiye. Since perlite is a non-hydrolysed material, water was used for the determination of their density.

The empty pycnometer with the capillary cap was dried at 25 °C and its weight was determined (A). Next, one fourth of the pycnometer was filled with the sample and its weight was once again measured (B). The pycnometer was subsequently slowly filled with water and shaken to ensure that no air bubbles remained between the particles. It was then dried at 25 °C together with the capillary cap and weighed (C). Finally, the pycnometer was emptied, dried at 25 °C, filled with water only, and its weight was determined with the capillary cap closed (D).

The true density, which was density of particles, was calculated using the formula given below where $\rho_{perlite}$ and ρ_{water} are the density values of the perlite sample and water, respectively.

$$\rho_{perlite} = \left(\frac{B-A}{(D-A)-(C-B)}\right) \times \rho_{water} \quad (1)$$

To determine the true density using a liquid pycnometer, the perlite samples with a particle size greater than 200 μm (a/Agricultural-expanded, b/Coarse-expanded, c/Fine-expanded, f/Coarse-unexpanded and g/Fine-unexpanded) were first ground with a vibratory disc mill (Retsch RS200). The similar liquid pycnometer methodology was previously used in the literature to measure particle density of cocopeat perlite mixtures (Ilahi and Ahmad, 2017). For these perlites, the results were obtained to be nearly constant.

The Brunauer-Emmet-Teller (BET) specific area of powdered perlite samples was measured using a Gemini® VII2390a analyzer at 77 K, under liquid nitrogen in Institute of Energy Technologies, Gebze Technical University, Gebze, Kocaeli, Türkiye. Before measurement, perlite samples were degassed under vacuum, at 120 °C for 2 hours (Kabra et al., 2013).

A Perkin Elmer 100 spectrometer was used to measure bending vibrations, asymmetric stretching, and symmetric stretching of bonds in perlite minerals. The Fourier-transformed infrared (FTIR) analysis was performed with 32 scans in 4000–400 cm^{-1} at a resolution of 1 cm^{-1}, with a diamond crystal universal attenuated total reflectance (UATR) accessory in Laboratory in the Department of Chemistry, Gebze Technical University, Gebze, Kocaeli, Türkiye.

Thermogravimetric analyses were performed on the perlite samples with use of a Q600-SDT thermal analyses, TA Instruments in Izmir Katip Çelebi University, Central Research Laboratories, Thermal Analysis Laboratory, Çiğli, Izmir, Türkiye. The temperature range of the test was between 30 and 1200 °C, and the heating rate was continuous 20 °C/min without intermediate step in nitrogen atmosphere with a flow rate of 50 mL/min.

3. Results and discussion

3.1. XRF analysis

In this research, quantity-based definition instead of the style often encountered in literature that highlights the origin of country, (Roulia et al., 2006; Kabra et al., 2013) was chosen. Convenient way for defining perlite mineral could be expressing ranges of quantity of ingredients in XRF tests similar to Nasrollahzadeh et al. work. Quantities was published in this paper by defining with the upper limit and lower limit. It's thought that XRF analysis must be performed for every specified amount of material in industry. The reason might be that even different perlite lodes in one mine might give different XRF results. XRF is very useful for understanding the production of expanded perlite, where there are many parameters such as exact origin of perlite mineral, chemical composition, which is directly related to XRF, effective water content, and initial particle size distribution. These were explained in papers of (Angelopoulos et al., 2013; Angelopoulos et al., 2014).

Content of "Fe" increased from "a" to "h" where “f, g, h” were pre-processed unexpanded perlites. Content of SiO_2 was around 75% in Table 1 and 2. However, in Reka et al's study content of SiO_2 was (72.48%), also Fe_2O_3 content was high (1.23%).

In tested samples of expanded perlites, the content of Na_2O was around 3%, in "b" sample it was as low as 2.52%. In unexpanded pre-processed perlites, in "f, g, h" samples, contents of Na_2O were rather different from expanded perlites, (1.36%), (1.50%) with the lowest values, in "h" sample content was the highest where value is (4.52%). In the study of Reka et al. (Reka et al., 2019) study Na_2O content was (3.56%). In the study of Reka and Adi-Darmawan, Na_2O content varied with lowest value at “1.87%” and highest value at (4.68%).

In tested perlites, content of Fe_2O_3 was the highest in "h" sample at “1.12%” value and was measured not below (0.56%) in "e" sample.

In literature (Reka et al., 2019)'s study; content of Fe_2O_3 was high (1.23%), while in (Adi-Darmawan et al., 2021)'s study content of Fe_2O_3 was above the average of tested samples of expanded and unexpanded/pre-processed perlites.

Contents of K_2O were around same values (4.12-4.81%) in both literature and tested samples. Among all tested samples, lowest SiO_2 (73.69%) with highest Na_2O (4.52%) content was observed in “h” perlite.

Al_2O_3 content was lower in literature around (13%) and higher in tested samples with (15-16%). The reason of these different percent ratios might be the different sources such as locations of mines and lodes. In "b, c, h" perlites, quantity of weight percentage of TiO_2 was close to zero - below detection limit.

This research's findings conformed to the research of (Roulia et. al., 2006) which proved that perlite could be thought as negatively charged aluminosilicate network stabilized with various metal cations. These findings will be discussed in next sections as XRD testing device does not detect minor contents that consist of small amounts of crystals. As seen in Table 1 and 2, oxides of Si, Al, Na, K could be detected.

Table 1. Chemical compositions of expanded and pre-processed perlites (weight % - powder method)

Content	a	B	c	d	e	f	g	h
SiO_2	75.58	75.14	75.31	75.26	75.68	75.24	75.59	73.69
Al_2O_3	15.56	15.50	15.62	15.36	15.33	16.04	16.04	15.25
Fe_2O_3	0.58	0.72	0.59	0.65	0.56	0.72	0.81	1.12
TiO_2	0.014	0- 0.0008	0- 0.0008	0.0049	0.096	0.016	0.189	0-0.00084
CaO	0.54	0.75	0.64	0.58	0.53	0.61	0.69	0.72
MgO	0.29	0.28	0.29	0.28	0.28	0.28	0.37	0.28
K_2O	4.12	4.81	4.25	4.27	4.01	4.44	4.46	4.12
Na_2O	2.99	2.52	3.03	3.24	3.33	1.36	1.50	4.52
Other	0.326	0.28	0.27	0.355	0.184	1.294	0.521	0.3
Total	100.0	100.0	100.0	100.0	100.0	100.0	100.0	100.0

Table 2. Chemical compositions of perlite in Reka et al., 2019; Adi-Darmawan et al., 2021 (weight %)

Content	Reka et al, 2019	Adi-Darmawan et al., 2021; Perlite Rock	Adi-Darmawan et al., 2021; Expanded Perlite
SiO_2	72.48	76.49	74.33
Al_2O_3	13.15	12.92	12.75
Fe_2O_3	1.23	0.93	0.95
TiO_2	0.15	0.12	0.15
CaO	1.13	0.92	2.10
MgO	0.35	0.13	0.88
K_2O	4.21	4.52	4.14
Na_2O	3.56	1.87	4.68
Other	3.74	2.1	0.02
Total	100.0	100.0	100.0

3.2. XRD analysis

The acquired XRD graphs for the pre-processed and expanded perlites, are given in Fig. 1. The variably humped pattern between approximately 15 and 35 ^{o} 2θ is assigned to the existence of amorphous groundmass.

As seen in Fig. 1, perlite samples were mostly observed in amorphous phases. In addition, some crystal phases were also observed. These crystal phases are symbolized as below:

Paragonite was abbreviated as "(P)" on graph, of which empirical formula is "$NaAl_2(AlSi_3)O_{10}(OH)_2$". Cristobalite was abbreviated as "(Cr)", of which empirical formula is "SiO_2". Quartz was shortened as "(Q)", which crystalline mineral is made up of "SiO_2". Albite was abbreviated as "(A)". Albite's empirical formula is "$Na(AlSi_3O_8)$". Illite was symbolized as "(I)". One of its composition could be given by formula $KAl_4(Si_7Al)O_{20}(OH)_4$.

As also stated in Materials section and Fig. 1, Agricultural-expanded “a”, coarse-expanded “b”, fine-expanded “c”, M1-expanded “d”, M3-expanded “e” trade named perlites were in expanded forms. Coarse-unexpanded “f”, fine-unexpanded “g”, and micronized-unexpanded “h” were trade names for “pre-processed” perlites, which were products of crushed raw perlite from the mine.

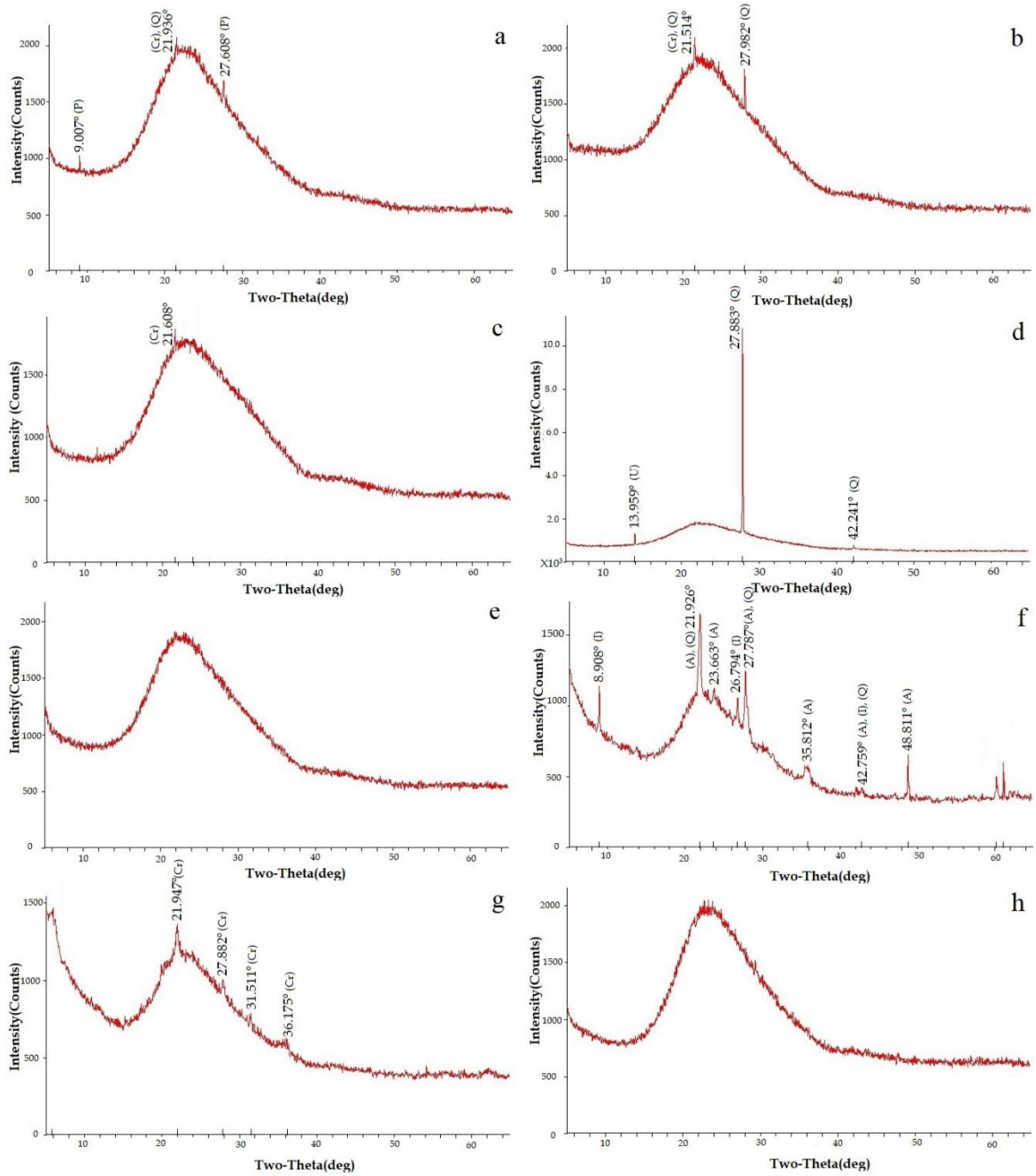

Fig. 1. XRD patterns of tested perlite samples. On upper right corner of each graph, type of perlite was explained (P: Paragonite, Cr: Cristobalite, Q : Quartz, A: Albite, I: Illite)

In this research, XRD characterization results generates similar amorphous characterization results that were confirmed with literature (Rostami-Vartooni et al., 2016; Xu et al., 2018; Saufi et al., 2020; Bian et al., 2021). It was observed that amorphous phase of expands of its original volume as explained in the study of (Roulia et al., 2006).

In coarse-unexpanded trade named "f" perlite; after XRD test, material was amorphous with crystal phases. It contained albite, illite, and quartz since it was coming from natural sources. Illite is potassium, alumina, silica hydrate containing alkali clay mineral. Albite is sodium, alumina, silicate containing feldspar phase. It's expected that these phases could exist in perlite.

Perlite is mainly amorphous material, and elements such as "potassium, sodium" fluxing agent behaving alkali elements could be transformed to melting phase. These elements could turn into amorphous phase depending on the cooling rate. Whether the perlite had little amorphous phase depends on heat treatment conditions besides chemical composition (Roulia et al., 2006).

In micronized-unexpanded trade named "h" perlite; no peaks were observed. This characterization was related with exact location of mine, and the lode that perlite was coming from. It could be concluded that all elements that were observed in XRF were in unordered network in amorphous phase.

3.3. Optical microscopy

In this research, optical microscopy provided an analysis for determining maximum particle size limits of perlite samples of expanded and unexpanded perlites. This could be possible with 400 μm scale in optical microscopy in Fig. 2. Particles with these size limits were visible in optical microscopy, and they were not seen on SEM.

In "a/agricultural-expanded", "b/coarse-expanded", "c/fine-expanded" samples, fine powders were observed because of pulverization in lab. In Fig. 2, "d/M1-expanded" perlite sample; 300-400 μm size particles were observed. "e/M3-expanded" perlite sample showed fine powders. "f/coarse-unexpanded" and "g/fine-unexpanded" perlite samples were unexpanded and contained perlite particles bigger than 400 μm. Size of particles were below 150 μm were visible and agglomerated forms were observed besides fine powders in Fig. 2- panel/sample "h/micronized-unexpanded" perlite.

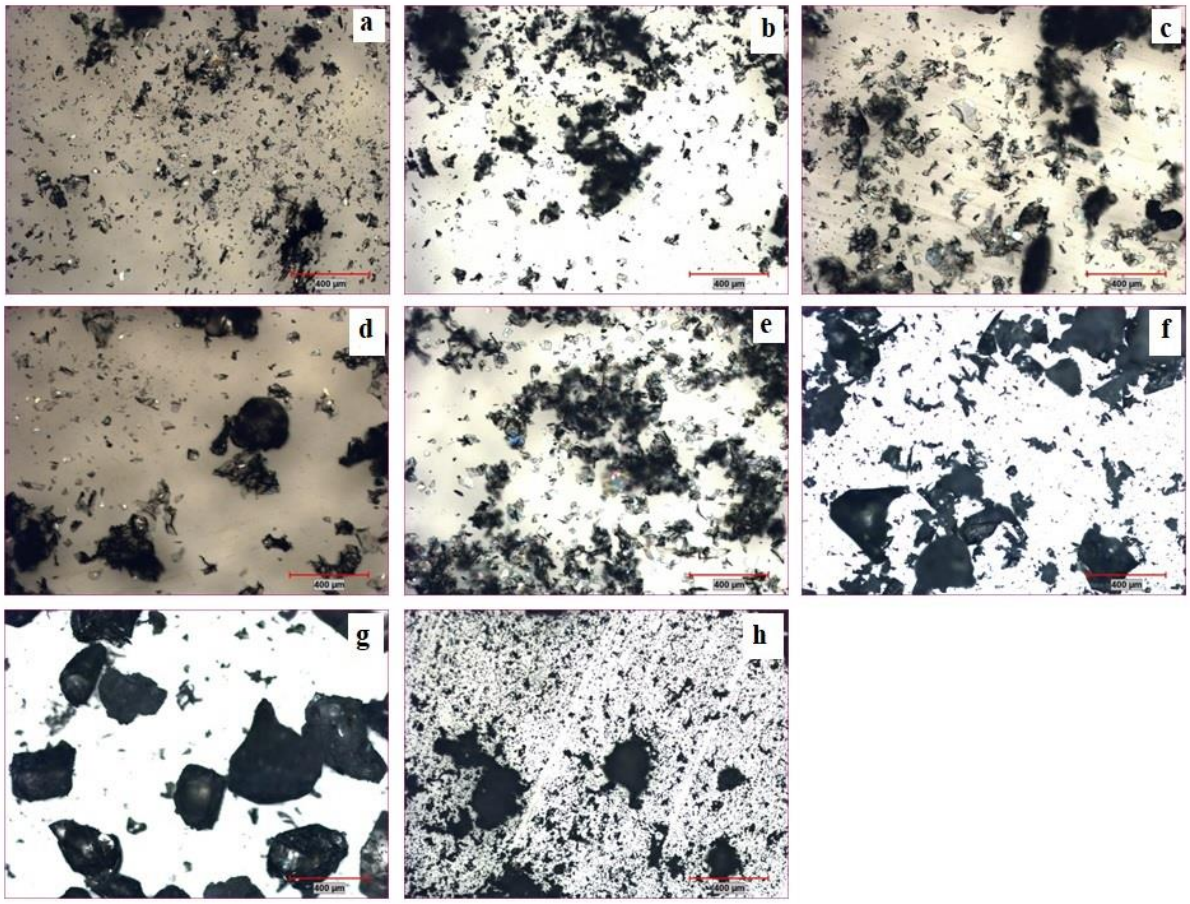

Fig. 2. Optical microscopy images of perlite samples and types of perlites were explained in upper right corner of each panel and materials section.

3.4. SEM observations

After observations had been obtained from optical microscopy for determining particle sizes and shapes, we used SEM to investigate the morphology of perlite samples in more detail (Fig. 3). In literature, this approach of optical microscopy to SEM analysis were also used (Palomar and Barluenga, 2018). Not-flake shaped perlites were observed in the pre-processed perlites f, g, and h.

While particles with a spongy and cracky shaped perlites were reported in several studies (Kaufhold et al., 2014; Gül, 2016; Pavlík and Bisaha, 2018; Vyšvařil et al., 2020), in this study flake-shaped perlites were observed as pulverized expanded perlites a, b, c, d, e in geometry wise. After obtaining from mine,

raw perlites were crushed to coarse, fine, and micronized form in second industrial facility where perlites keep their unexpanded form. Then they were expanded by fast heating in a third expanded perlite manufacturing factory ("Kaleperlit" for our samples), forming foamy or spongy expanded perlites. Then walls that make up the expanded perlite foams could form flake-shaped particles or perlite membranes by sieving in factory and pulverization in lab.

The reason of flake-shaped perlite geometries in the SEM images of the samples "a, b, c, d and e" might be the processing conditions such as sieving in industrial manufacturing and pulverization that were carried out in laboratory.

In ongoing research (unpublished), when these perlites were mixed with biopolymers to form biocomposites; morphology, shape, true density, mechanical properties of perlite played major role in determining the final properties these polymer biocomposites.

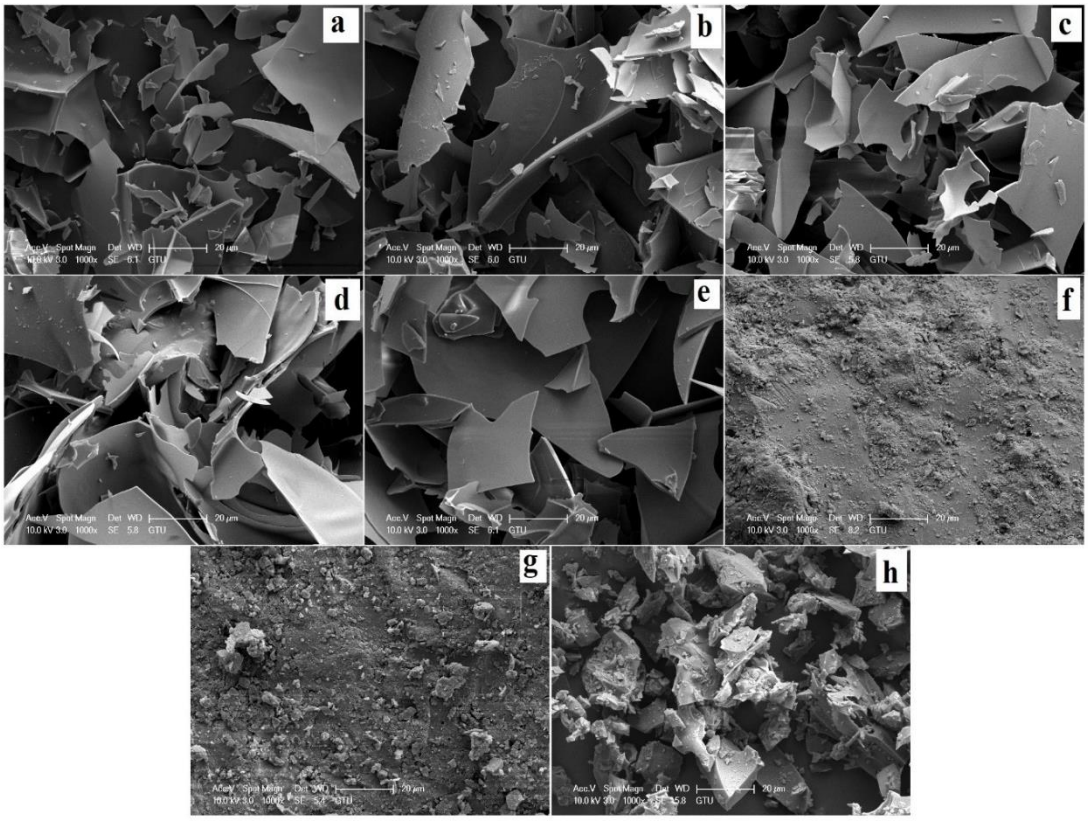

Fig. 3. Secondary electron images from perlite samples at 1000x magnifications

3.5. Density

The true density was found to be in the range of 2.31–2.45 g/cm^3 for all samples except "d/M1-expanded", "e/M3-expanded" and "h/Micronized-unexpanded" perlites which were different (Table 3). The grinding was not performed for these samples before measuring true density. The reason was that "d/M1-expanded", "e/M3-expanded", and "h/Micronized-unexpanded" perlites were smaller than 200 µm. Especially the density values of "d/M1-expanded" and "e/M3-expanded", which had different particle sizes, were lower than the others since these commercial perlites, were in the expanded form. They contained voids, which are probably the main reason of the lower densities of "d/M1-expanded" and "e/M3-expanded"."h/Micronized-unexpanded" perlite was crushed in second stage industrial facility as explained in previous sections that the "h/Micronized-unexpanded" material was between 0 and 150 µm in size. Particle size range of "h/Micronized-unexpanded" was different from particle sizes of pre-processed perlites as seen optical microscopy. This might be the reason of true density differences of "h/Micronized-unexpanded" perlite and "f/Coarse-unexpanded", "g/Fine-unexpanded" perlites. In this research, true density was measured because these values were directly used in micromechanical modelling for Young modulus prediction and manufacturing of polymer biocomposites in on-going research.

Table 3. True density of perlites

Perlite Samples	Density (g/cm^3)
a/Agricultural-expanded	2.45
b/Coarse-expanded	2.31
c/Fine-expanded	2.35
d/M1-expanded	0.84
e/M3-expanded	1.34
f/Coarse-unexpanded	2.39
g/Fine-unexpanded	2.44
h/Micronized-unexpanded	2.00

3.6. BET surface area analysis

BET analysis was used to determine the surface areas of the perlite samples, which were measured between 1–3 m^2/g (Table 4). The total surface area values of expanded perlites were reported as the highest for samples ”a” (2.99 m^2/g) and ”c” (2.65 m^2/g). Except for ”d”, the total surface areas of the expanded perlites were higher than those of the pre-processed perlites. Sample “d” had a lower surface area because it had a lower density, so it had a lower mass per unit volume. Similar surface area values for perlite samples were published in several previous studies (Bastani et al., 2006; Torab-Mostaedi et al., 2010; Kabra et al., 2013). On the other hand, surface areas greater than 5 m^2/g were also reported in the literature due to different processing, physical conditions, and origin of mines as stated in studies of (Srivastava et al., 2013; Wang et al., 2015; Bian et al., 2021; Adi-Darmawan et al., 2021).

Table 4. BET surface area values of perlites

Perlite Samples	Total Surface Area (m^2/g)
A	2.99
B	1.97
C	2.65
D	1.21
E	2.10
F	1.68
G	1.83
H	1.12

3.7. FTIR analysis

In FTIR analysis, qualitative analysis and for some in-depth studies quantitative analysis can be conducted. In this work, qualitative analyses were carried out demonstrating the related bonds in perlite materials showing the related bands from FTIR graphs.

FTIR spectra of all perlite samples showed absorption bands at 780, 1000 and 1628 cm^{-1} (Fig. 4). The peaks observed in the range 770 – 788 cm^{-1} (Table 5) were a result of stretching vibrations of Si-O groups. The band at approximately 1000 cm^{-1} was due to stretching vibrations in the Si-O-M (M: Al or Si) groups. It was observed that the Si-O symmetric and asymmetric stretching bands had approximate values, and they were similar to those of previous studies (Cabuk et al., 2018; Bilgiç and Bilgiç, 2019). The transmittance values of all expanded perlites and pre-processed ”h” perlite at 780 and 1000 cm^{-1} were similar and higher than the corresponding values for “f” and ”g”.

The peaks around 1628 cm^{-1} (between 1600-1650 cm^{-1}) were attributed to bending vibrations of O-H groups originating from water molecules (Cabuk et al., 2018; Bilgiç and Bilgiç, 2019; Reka et al., 2019; Saufi et al., 2020). It was observed that expanded perlite “a” had a lower O-H band than other perlites due to its lowest water content. The results of the FTIR analysis were in good agreement with previous studies (Kabra et al., 2013; Edebali, 2015; Cabuk et al., 2018; Bilgiç and Bilgiç, 2019; Reka et al., 2019; Saufi et al., 2020).

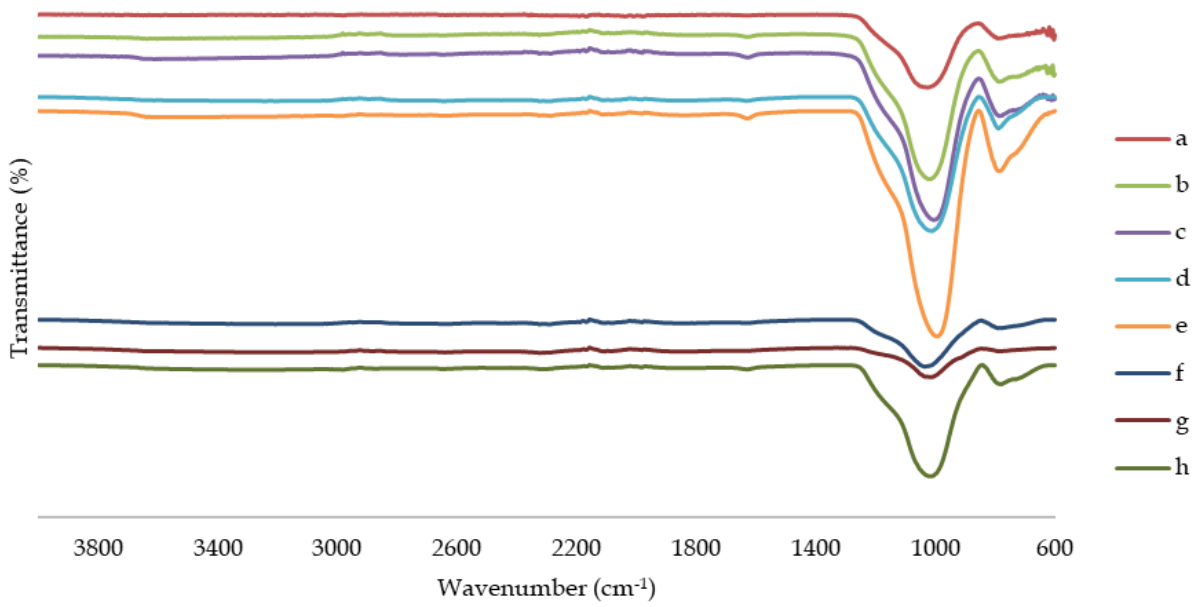

Fig. 4. FTIR spectra of expanded and pre-processed perlite samples

Table 5. FTIR results of perlites

Perlite Samples	O-H bending vibration	Si-O-Si vibration (asymmetric stretching)	Si-O-Si vibration (symmetric stretching)
A	1624.5	1018.6	783.3
B	1628.3	1020.6	784.9
C	1630.1	1004.4	786.2
D	1632	1009.3	788
E	1628.3	991.3	783.5
F	1628.3	1035.6	778.1
G	1628.3	1011.6	-
H	1628.3	1011.7	777.2

3.8. TGA

The TGA results of the five expanded and three unexpanded/pre-processed perlite samples examined are shown in Fig. 5. It was observed that the weight losses of the expanded perlites were between 0.5–2.5%, and the weight losses of pre-processed perlites ”f, g, h” were between 2.5–5.0%.

In the first temperature range (0–250 °C), the weight losses were attributed to the removal of moisture absorbed by the perlite surface breaking of H-bonds between water and silicate chains. According to examinations, the weight losses in the range of approximately 250-500 °C indicated the dehydroxylation of remaining chemically bonded water in the samples. Based on the TGA results, the weight losses of expanded perlites occurred in the first temperature range, while the weight losses of pre-processed perlites occurred in the second temperature ranges. This difference was probably related to the expansion ability of perlite. As a result of this ability, weight losses were observed due to the release of molecular water in the closed cell pores of raw perlites with the increase in temperature during the test (Kabra et al., 2013; Gül, 2016; Cabuk et al., 2018; Reka et al., 2019).

Previous studies that performed thermogravimetric analysis of pre-processed perlites reported that 2–5% of the sample corresponded to the volatile content (Barker et al., 2006; Gül, 2016; Haery, 2017). In this study, 4.81%, 2.76% and 3.62% of the samples belonged to the volatile content for ”h”, ”f”, and ”g” perlites, respectively. The reasons for the weight loss in current samples could be loss of moisture and also thermal decomposition according to a previous study of (Cabuk et al., 2018).

In Fig. 5, positive slopes were observed after 800 °C on the samples ”b” and ”c”. The reason might be due to oxidation during the heating process.

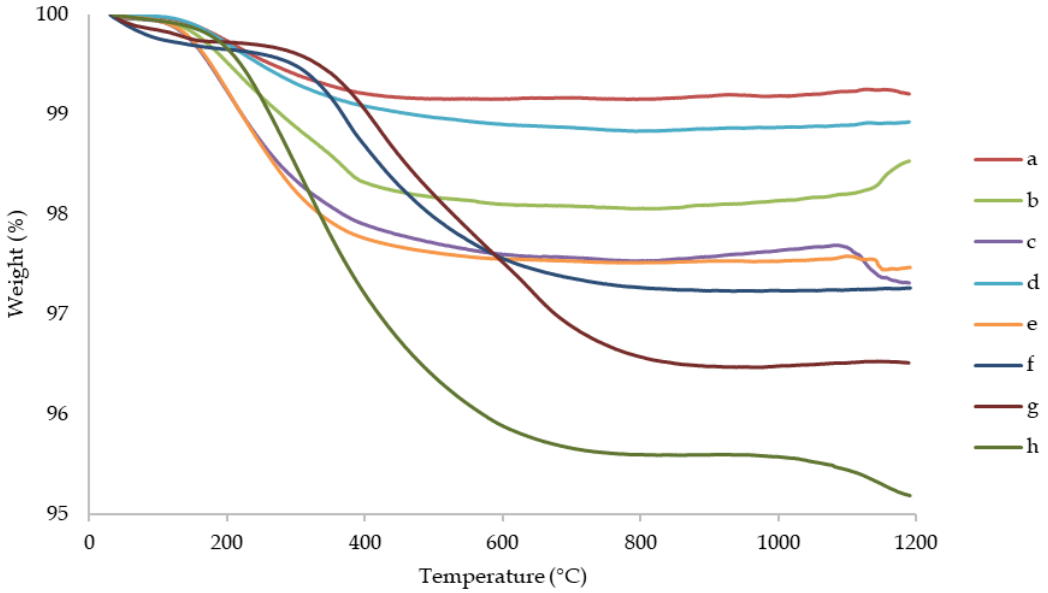

Fig. 5. TGA results of all perlite samples (94-100 wt%)

Table 6. Amount of volatile content on different types of expanded perlites

Expanded Perlite Samples	% Amount of Volatile Content
A	0.84
B	1.93
C	2.68
D	1.15
E	2.54

4. Conclusions

Various minerals are commonly used in polymers as additives and/or fillers. Perlite is found in large quantities in Türkiye and among many rocks on earth, perlite is one of them having various application areas including polymers as a potential new area. We characterized eight different perlite samples from the Bergama Izmir region using a wide range of analytical techniques and compared the obtained results in a very comprehensive way.

While XRF analysis revealed that the perlite minerals have similar chemical compositions, XRD analysis showed that during expansion process crystals were transformed to amorphous structure. In expanded perlites, highly amorphous, less crystal phases were observed with detailed results. Crystal phases had better mechanical properties than amorphous phases. These results confirmed that expanded perlite samples were soft type of perlites. The crystallinity change was also confirmed by BET analysis showing that highly crystalline perlite minerals have lower surface area. In morphological analysis, upper limits of particles are visible on optical microscopy and details of particles are seen with SEM. In literature, foamy images of expanded perlites were seen. On the contrary, flake shaped expanded perlites were observed in our samples which might prove the theory that flake shaped expanded perlites could be new types of reinforcement materials for polymer biocomposites. In TGA, it was concluded that weight loss was related to dehyroxylation of chemically bonded water and burning of organic constituents.

Depending on the crystallinity, chemical composition, and morphology of perlite materials, three of them were selected to be used in on-going biopolymer and biocomposite research to obtain sustainable composites using perlite materials. In a previous conference proceeding, some preliminary results on polylactic acid and perlite composites were demonstrated (Aksoy et al., 2021). With this in-depth information on perlite characterization, in-depth research using these data on perlite materials will

enlighten the biopolymer research in the group. Furthermore, this study highlights these fundamental properties to be used in not biopolymers but also in many different polymer composite systems.

Acknowledgements

Authors would like to thank Çağatay Doğan from Agropas Trade for his discussions on perlite minerals, and Izmir Katip Çelebi University BAP 2021-TDR-FEBE-0005 Ph.D. thesis support for funding.

References

ADI DARMAWAN, DIDIT, WAHYUDI, AGUS, ERIC MAMBY, HASUDUNGAN, SUHERMAN, IJANG, 2021. *Characterization of perlite and expanded perlite from West Sumatera, Indonesia*, *IOP Conference Series: Earth and Environmental Science*, 882(1), 012010.

AKSOY, ÖZAY, MOCAN, MERVE, YÜCETÜRK, MERT, ALYAMAÇ, ELIF, AYDIN, LEVENT, GÜRSOY, BAHADIR, SEYDIBEYOĞLU, M. ÖZGÜR, 2021. *Manufacturing and Characterization of Perlite Biocomposites*, International Pumice and Perlite Symposium, Pupes 21., e-ISBN:978-605-71070-0-8, 38-42.

ANGELOPOULOS, PANAGIOTIS M., GEROGIORGIS, DIMITRIOS I., PASPALIARIS, IOANNIS, 2013. *Model-based sensitivity analysis and experimental investigation of perlite grain expansion in a vertical electrical furnace*, Industrial and Engineering Chemistry Research, 52(50), 17953–17975.

ANGELOPOULOS, PANAGIOTIS M., GEROGIORGIS, DIMITRIOS I., PASPALIARIS, IOANNIS, 2014. *Mathematical modeling and process simulation of perlite grain expansion in a vertical electrical furnace*, Applied Mathematical Modelling, 38(5–6), 1799–1822.

BARKER, J.M. SANTINI, K., 2006. '*PERLITE*', IN J.E. KOGEL, N.C. TRIVEDI, J.M. BARKER, S.T.K., ed.. *Industrial Minerals and Rocks - Commodities, Markets, and Uses*. Society for Mining, Metallurgy, and Exploration, SME., 685–702.

BASTANI, D., SAFEKORDI, A. A., ALIHOSSEINI, A., TAGHIKHANI, V., 2006. *Study of oil sorption by expanded perlite at 298.15 K*, Separation and Purification Technology, 52(2), 295–300.

BIAN, YADONG, WANG, KEJIAN, WANG, JULIAN, YU, YONGSHENG, LIU, MINGYUE, LV, YAJUN, 2021. *Preparation and properties of capric acid: Stearic acid/hydrophobic expanded perlite-aerogel composite phase change*, Renewable Energy, 179, 1027–1035.

BILGIÇ, CEYDA, BILGIÇ, ŞAFAK, 2019. *Application of Fourier Transform Infrared, FTIR. Spectroscopy to Analysis of Clays*, Nevşehir Bilim ve Teknoloji Dergisi, 8(20 19), 37–46.

BÜLBÜL, KADIR, 2022., http://www.kaleperlit.com.tr/(Accessed: 3 Jan 2022.

CABUK, MEHMET, YESIL, TOLGA ACAR, YAVUZ, MUSTAFA, UNAL, HALIL IBRAHIM, 2018. *Colloidal and viscoelastic properties of expanded perlite dispersions*, Journal of Intelligent Material Systems and Structures, 29(1., 32–40.

CHEN, FEIXU, ZHANG, YIHE, LIU, JINGANG, WANG, XINKE, CHU, PAUL K., CHU, BOHUA, ZHANG, NA, 2020. *Fly ash based lightweight wall materials incorporating expanded perlite/SiO2 aerogel composite: Towards low thermal conductivity*, Construction and Building Materials, 249, 118728.

EDEBALI, SERPIL, 2015. *Alternative Composite Nanosorbents Based on Turkish Perlite for the Removal of Cr(VI. from Aqueous Solution*, *Journal of Nanomaterials*, 2015, 18–20.

ERDEM, T. K., MERAL, Ç, TOKYAY, M., ERDOĞAN, T. Y., 2007. *Use of perlite as a pozzolanic addition in producing blended cements*, Cement and Concrete Composites, 29(1), 13–21.

GÜL, DILEK, 2016. C*haracterization and Expansion Behaviour of Perlite*, (July), 1–94.

HAERY, HALEH ALLAMEH, 2017. *Elastic And Mechanical Properties Of Expanded Perlite And Perlite/Epoxy Foams*.

ILAHI, WAN FAZILAH FAZLIL, AHMAD, DESA, 2017. *A study on the physical and hydraulic characteristics of cocopeat perlite mixture as a growing media in containerized plant production*, Sains Malaysiana, 46(6), 975–980.

JAMEI, M., GUIRAS, H., CHTOUROU, Y., KALLEL, A., ROMERO, E., GEORGOPOULOS, I., 2011. '*Water retention properties of perlite as a material with crushable soft particles*', *Engineering Geology*, 122(3–4), 261–271.

KABRA, SAKSHI, KATARA, STUTI, RANI, ASHU, 2013. *Characterization and Study of Turkish Perlite*, International Journal of Innovative Research in Science, Engineering and Technology, 2(9), 4319–4326.

KAUFHOLD, STEPHAN, REESE, ANKE, SCHWIEBACHER, WERNER, DOHRMANN, REINER, GRATHOFF, GEORG H., WARR, LAURENCE N., HALISCH, MATTHIAS, MÜLLER, CORNELIA, SCHWARZ-SCHAMPERA, ULRICH, UFER, KRISTIAN, 2014. *Porosity and distribution of water in perlite from the island of Milos, Greece*, Journal of the Korean Physical Society, 3(1), 1–10.

MAXIM, L. DANIEL, NIEBO, RON, MCCONNELL, ERNEST E., 2014. *Perlite toxicology and epidemiology - A review*, Inhalation Toxicology. Informa Healthcare, 259–270.

NASROLLAHZADEH, MAHMOUD, SAJADI, S. MOHAMMAD, ROSTAMI-VARTOONI, AKBAR, BAGHERZADEH, MOJTABA, SAFARI, REZA, 2015. *Immobilization of copper nanoparticles on perlite: Green synthesis, characterization and catalytic activity on aqueous reduction of 4-nitrophenol*, Journal of Molecular Catalysis A: Chemical, 400, 22–30.

PALOMAR, I., BARLUENGA, G., 2018. *A multiscale model for pervious lime-cement mortar with perlite and cellulose fibers*, Construction and Building Materials, 160, 136–144.

PAPADOPOULOS, ATHANASIOS P., BAR-TAL, ASHER, SILBER, AVNER, SAHA, UTTAM K., RAVIV, MICHAEL, 2008. *Inorganic and synthetic organic components of soilless culture and potting mixes*, Soilless Culture: Theory and Practice.

PAVLÍK, VLADIMÍR, BISAHA, JURAJ, 2018. *Lightweight mortars based on expanded perlite*, Key Engineering Materials, 776 KEM, 104–117.

REKA, ARIANIT A., PAVLOVSKI, BLAGOJ, LISICHKOV, KIRIL, JASHARI, AHMED, BOEV, BLAZO, BOEV, IVAN, LAZAROVA, MAJA, ESKIZEYBEK, VOLKAN, ORAL, AYHAN, JOVANOVSKI, GLIGOR, MAKRESKI, PETRE, 2019. *Chemical, mineralogical and structural features of native and expanded perlite from Macedonia*, Geologia Croatica, 72(3), 215–221.

ROSTAMI-VARTOONI, AKBAR, NASROLLAHZADEH, MAHMOUD, ALIZADEH, MOHAMMAD, 2016. *Green synthesis of perlite supported silver nanoparticles using Hamamelis virginiana leaf extract and investigation of its catalytic activity for the reduction of 4-nitrophenol and Congo red*, Journal of Alloys and Compounds, 680, 309–314.

ROULIA, M., CHASSAPIS, K., KAPOUTSIS, J. A., KAMITSOS, E. I., SAVVIDIS, T., 2006. *Influence of thermal treatment on the water release and the glassy structure of perlite*, Journal of Materials Science, 41(18), 5870–5881.

SAUFI, HAMID, EL ALOUANI, MAROUANE, ALEHYEN, SALIHA, EL ACHOURI, MOHAMMED, ARIDE, JILALI, TAIBI, M'HAMED, 2020. *Photocatalytic Degradation of Methylene Blue from Aqueous Medium onto Perlite-Based Geopolymer*, International Journal of Chemical Engineering, 2020.

SRIVASTAVA, KHUSHBOO, SHRINGI, NIHARIKA, DEVRA, VIJAY, RANI, ASHU, 2013. *Pure Silica Extraction from Perlite: Its Characterization and Affecting factors*, International Journal of Innovative Research in Science, Engineering and Technology, 2(July)

TORAB-MOSTAEDI, M., GHASSABZADEH, H., GHANNADI-MARAGHEH, M., AHMADI, S. J. AND TAHERI, H., 2010. *Removal of cadmium and nickel from aqueous solution using expanded perlite*, Brazilian Journal of Chemical Engineering, 27(2), 299–308.

WANG, XUEJIANG, WANG, XIN, WANG, WEI, ZHANG, JING, ZHAO, JIANFU, GU, ZAOLI AND ZHOU, LIJIE, 2015. *Synthesis, structural characterization and evaluation of floating B-N codoped TiO 2 /expanded perlite composites with enhanced visible light photoactivity*, Applied Surface Science, 349, 264–271.

XU, HAIYAN, JIA, WEIHONG, REN, SILI, WANG, JINQING, 2018. *Novel and recyclable demulsifier of expanded perlite grafted by magnetic nanoparticles for oil separation from emulsified oil wastewaters*, Chemical Engineering Journal, 337(December 2017), 10–18.

YILMAZER, SEMIHA, OZDENIZ, MESUT B., 2005. *The effect of moisture content on sound absorption of expanded perlite plates*, Building and Environment, 40(3), 311–318.